

ADAPTIVE MESH REFINEMENT FOR PARTICLE-TRACKING CALCULATIONS

J. DeFord, B. Held, Simulation Technology & Applied Research, Inc., Mequon, WI 53092, U.S.A.
J. J. Petillo, Science Applications International Corp., Burlington, MA 01813, U.S.A.

Abstract

Particle orbit errors in multipacting and dark current computations can arise from inadequate field representation, poor surface modeling, and from the integration algorithm used to advance the particles. Established fields-based adaptive mesh refinement (AMR) methods selectively improve the field and surface representation over several iterations in finite-element codes but they are not optimized for particle tracking. In particular, field emission and secondary emission models require precise surface representations and highly accurate field representations near surfaces, and these requirements are not adequately addressed in standard AMR techniques. In this paper we report on extensions to existing AMR support in the Analyst software package for particle tracking, including adaptive improvement of near-surface and on-surface field representations. We present the application of two mesh refinement metrics to AMR in multipacting and gun code calculations. It is shown that the methods yield a rapidly convergent value for the electron gun current. In the multipacting computation example, additional resonances are uncovered that were not evident in the initial mesh.

INTRODUCTION

Adaptive mesh refinement is an important practical aspect of finite-element analysis. Finite-element solutions improve via global refinement of the mesh, but such refinement is computationally prohibitive in most cases so various approaches to local mesh improvement have been developed. Local error estimates guide most electromagnetic fields-based AMR methods, typically yielding substantially more accurate results for a given unknown count than uniformly refined meshes will [1,2].

In a typical approach to AMR an element in the finite-element mesh is given a score based upon the expression

$$f_k = \frac{e_k}{E}$$

where e_k is the error estimate for the k -th element, typically based upon local violations of the Maxwell equations, and E is a normalization factor, e.g., the maximum of the element errors across the mesh, or a maximum acceptable error. An element is then selected for refinement if its score exceeds a specified value, which is used to control the rate of growth in the element count with each AMR iteration. The element score can also be used to identify regions where the elements can be made larger without introducing excessive errors.

In computations involving particles there are potentially a variety of errors associated with the particles themselves, in addition to the usual field errors. For tracking codes such as the PT3P solver in Analyst, the primary sources of particle errors are field representation on an element, which affects integration accuracy, and surface representation, which affects surface fields and consequently emission processes. A robust mesh refinement algorithm must consider both of these effects. In this paper we introduce two metrics to account for particles in the AMR process and apply these metrics to two common types of tracking problems.

PARTICLE-BASED AMR

To incorporate particle errors into the AMR process in Analyst we first use the local field errors, as determined by the field solver, to generate a list of elements for refinement that improves the field representation. The particles are tracked on the same mesh that is used for the field solve, and after the particle calculation we generate a list of elements to be refined based upon estimated tracking errors. The two lists are then combined to form a composite set that is used for mesh refinement.

We considered two different metrics for the effective element error due to particles: (1) a count of the number of particle tracks that traverse the element ($e_k = P_k$), and (2) the number of particle track knots that are located within an element ($e_k = N_k$). The former is a measure of the total particle population traversing the element, with elements having relatively large populations being subdivided before elements with few or no particles. The latter metric measures how complex the particle orbits are within an element, with complex motion resulting in more internal knots due to integration requirements. For the purposes of this study the normalization factor E was set to the largest value of e_k , and the number of elements subdivided at each AMR iteration was constrained to be a fixed fraction of the total number of elements in the mesh.

SNS HOM CAVITY EXAMPLE

To assess the efficacy of error metrics discussed above we modeled a SNS HOM (high beta) cavity under study at FNAL[3] (see Fig. 1). The second mode in this structure resonates around 810 MHz and exhibits multipacting from the antenna to the surrounding walls over a range of field levels [4].

The initial coarse mesh is shown in Fig. 2. In this mesh the antenna and the surrounding region are very poorly

represented. The AMR loop was then run for 4 iterations, and the final mesh is shown in Fig. 3. At each iteration, the mesh was first refined using the element refinement list generated on the previous iteration, then an eigensolve was performed with OM3P[5,6], followed by a particle solve using PT3P.

The resulting average yield function curves using the orbit complexity metric $e_k = N_k$ for 291 field levels up to 30 MV/m are shown in Fig. 4, with the field level referring to the peak axial electric field on the cavity axis. The average yield function is defined as

$$YF_{ave} = \frac{\sum_{i=1}^{N_r} \exp[\log(Y_i)/M]}{N_r}$$

where the sum is carried out only over resonant particles, Y_i is the cumulative secondary emission yield (after M impacts) of the i -th particle, and N_r is the total number of resonant particles. Both the eigensolve and the particle analysis were run on a 16 processor Linux cluster, resulting in a total elapsed run time of 43 hours. A total of 4.9×10^8 particle tracks were computed.

The initial mesh shows significant errors, with the resonance at high field strength missed altogether, and resonances at lower field levels shifted from their proper locations. Subsequent meshes show good convergence to a final solution, particularly for the first two resonances, that is consistent with available measured data on this structure[4]. All resonant particles at three different field levels are shown in Fig. 5, showing distinct regions where multipacting is occurring.

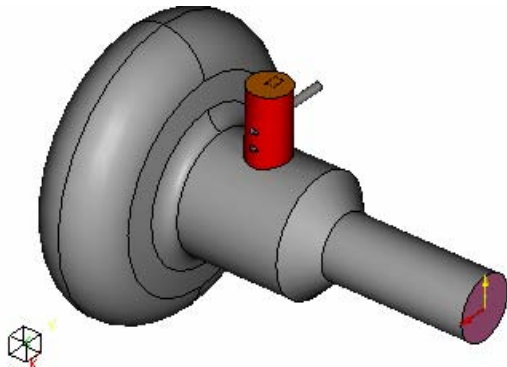


Fig. 1. SNS HOM cavity.

A similar AMR progression is seen when the metric $e_k = P_k$ is used.

APPLICATION TO GUN PROBLEM WITH MICHELLE CODE

The particle population metric $e_k = P_k$ has been implemented in the MICHELLE[7] code, and we have used this approach to model electron guns. The gun

model we analyzed consisted of a spherical cathode, an anode, and a drift section, and the initial mesh is shown in Fig. 6. MICHELLE is used to compute the steady-state beam distribution within the device including the effects of static external fields and space charge/current. The beam is unconfined in the drift tube, so it expands as it drifts through this section.

The AMR process was run for a total of 8 iterations. A slice of the final mesh through the axis of the gun is shown in Fig. 7, showing the refinement in the vicinity of the beam. No additional refinement was done to improve the field representation, although this is an option in the MICHELLE code.

The results of the AMR progression are shown in Fig. 8. The rapid convergence of a key gun parameter (the total gun current) with increasing iteration number is evident.

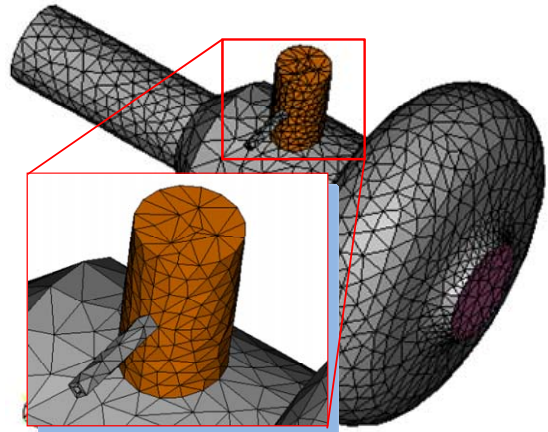


Fig. 2. Initial mesh with 33K tetrahedrons.

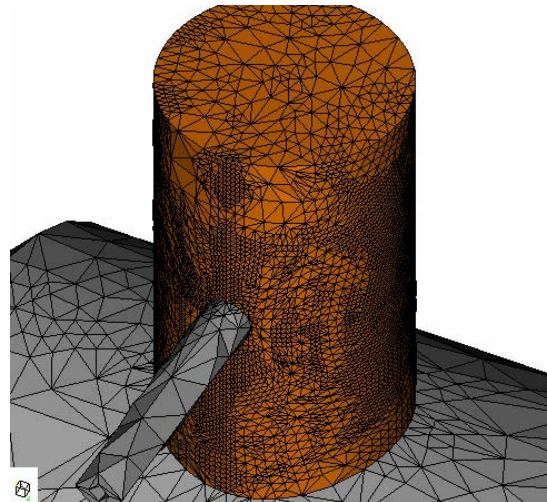


Fig. 3. Closeup of SNS cavity antenna housing for final mesh in AMR progression using orbit complexity metric.

CONCLUSIONS

We report on two metrics for use in guiding adaptive mesh refinement for particle tracking calculations: one metric is a measure of the total number of particles that traverse an element, and the other measures the

complexity of the particle orbits within an element. The former was applied to the analysis of a gun, and the latter to multipacting in an RF cavity. The results of these computations suggest that both metrics have merit, in both cases achieving significant improvement in accuracy and result detail as compared to coarse initial meshes.

REFERENCES

[1] G. Drago, et al., IEEE Trans. on Mag., **28**, 1992, pp. 1743-1746.
 [2] D. K. Sun, et al., IEEE Trans. on Mag., **36**, July 2000, pp. 1596-1599.
 [3] I. Gonin, FNAL, private communication.
 [4] I. Gonin, et al., WEPMN093, proceedings this conference.
 [5] J. DeFord et al., Proc. of PAC 2003, Portland, OR, pp. 3554-3556.
 [6] J. DeFord et al., Proc. of ICAP 2002, East Lansing, MI, pp. 57-62.
 [7] J. Petillo, et al., IEEE Trans. Plasma Sc., **30**, June, 2002, pp. 1238-1264.

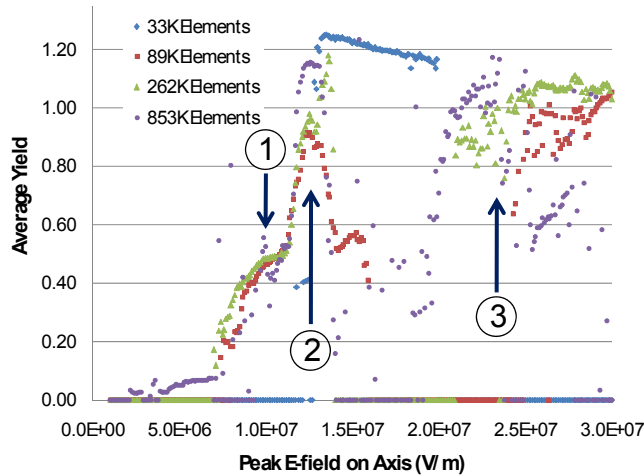


Fig. 4. Average field function for each mesh in the AMR progression for the SNS cavity. Numbers indicate location of multipactor (see Fig. 5).

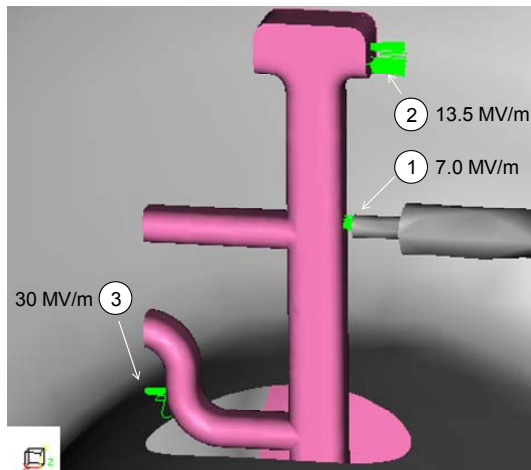


Fig. 5. Multipacting particle orbits for three levels of peak axial electric field (the orbits at 13.5 MV/m and 30 MV/m terminate on antenna housing which is not shown).

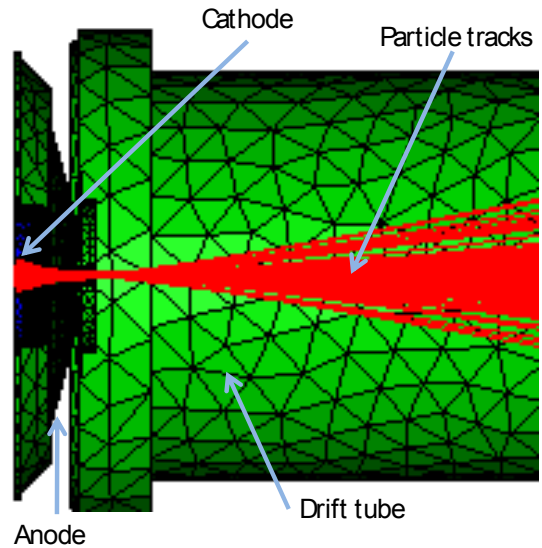


Fig. 6. Surface of initial mesh of electron gun and drift tube, with corresponding electron trajectories.

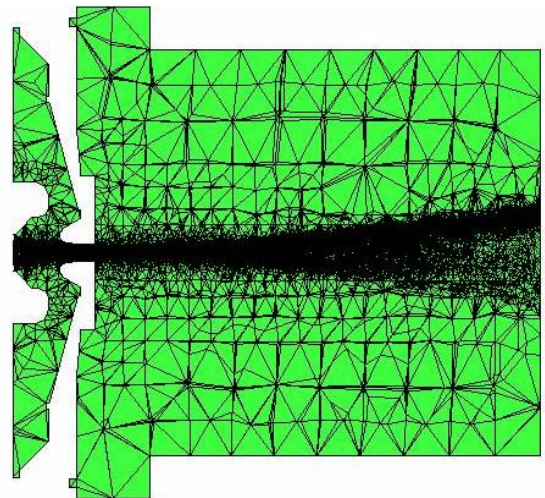


Fig. 7. Cut of mesh along axis of gun model for AMR iteration 7 (4.3M elements). Note concentration of elements in vicinity of beam in A-K gap and in drift region where beam is unconfined.

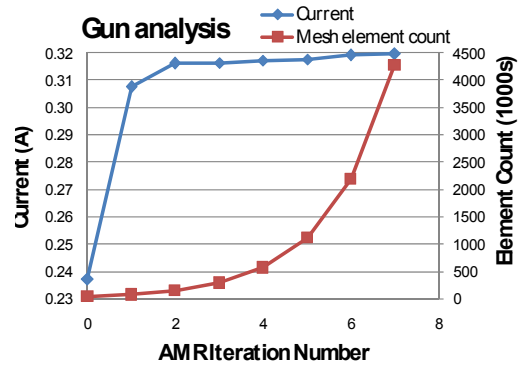


Fig. 8. AMR progression for MICHELLE analysis of electron gun.